Scientia Agricola

# Process-based simple model for simulating sugarcane growth and production

Fábio R. Marin[1,§]*, James W. Jones[2]

[1]Embrapa Agricultural Informatics, Av. André Tosello, 209, Barão Geraldo, C.P. 6041 – 13083-886 – Campinas, SP – Brazil.
[2]University of Florida – Dept. of Agricultural and Biological Engineering, PO Box 110570, Museum Road, 32611 – Gainesville, Florida – USA.
*Corresponding author <fabio.marin@usp.br>

Edited by: Paulo Cesar Sentelhas

*Received August 22, 2012*
*Accepted June 06, 2013*

ABSTRACT: Dynamic simulation models can increase research efficiency and improve risk management of agriculture. Crop models are still little used for sugarcane (*Saccharum* spp.) because the lack of understanding of their capabilities and limitations, lack of experience in calibrating them, difficulties in evaluating and using models, and a general lack of model credibility. This paper describes the biophysics and shows a statistical evaluation of a simple sugarcane process-based model coupled with a routine for model calibration. Classical crop model approaches were used as a framework for this model, and fitted algorithms for simulating sucrose accumulation and leaf development driven by a source-sink approach were proposed. The model was evaluated using data from five growing seasons at four locations in Brazil, where crops received adequate nutrients and good weed control. Thirteen of the 27 parameters were optimized using a Generalized Likelihood Uncertainty Estimation algorithm using the leave-one-out cross-validation technique. Model predictions were evaluated using measured data of leaf area index, stalk and aerial dry mass, and sucrose content, using bias, root mean squared error, modeling efficiency, correlation coefficient and agreement index. The model well simulated the sugarcane crop in Southern Brazil, using the parameterization reported here. Predictions were best for stalk dry mass, followed by leaf area index and then sucrose content in stalk fresh mass.

## Introduction

Dynamic simulation models can increase research efficiency by allowing the analyst to search for strategies and analyze system performance, improve risk management, and interpret field experiments that deal with crop responses to soil, management, genetic or environmental factors (Keating et al., 1999).

Sugarcane (*Saccharum* spp.) is of major social and economic importance in Brazil. Worldwide, there have been several models developed specifically for sugarcane crop simulation (Pereira and Machado, 1986; Jones et al., 1989; Langellier and Martine, 2007; Keating et al., 1999; Thorburn et al., 2005; Inman-Bamber, 1991; Singels et al., 2008).

Some of the physiological development and growth parameters that appear in the functions vary among sugarcane cultivars, meaning that they have to be estimated from data in order to predict growth and yield. Some of the parameters cannot be measured directly in typical experiments; instead, they have to be estimated based on data that are measured in experiments. Recent literature contains relatively little work on parameter estimation for crop models (Ahuja and Ma, 2011; Makowski et al., 2006). Makowski et al. (2006) point out the importance of raising the quality of calibration in crop models with automatic procedures for parameter adjustment. This would help ensure that the data are always used appropriately and in the same way for parameter estimation (Wallach et al., 2001), but such procedures are not available for direct use with existing sugarcane models.

A new sugarcane model was developed that builds on well-tested relationships used in existing models, adding new features (such as for photosynthesis, leaf development driven by a source-sink approach, and sucrose accumulation algorithms) based on recent literature and experiments. This new model also incorporates an objective calibration procedure based on Generalized Likelihood Uncertainty Estimator (GLUE) to ensure consistent and reliable adaptation of the model for applications in Brazil. The purpose of this paper is to describe the functional basis of this simple model and to evaluate it for an important Brazilian cultivar studied in a latitudinal range in Southern Brazil, with a diverse range of planting dates, soils and water availability.

## Materials and Methods

### Model Description

The model simulates sugarcane growth and development using process-based algorithms including phenology, canopy development, tillering, biomass accumulation and partitioning, root growth, and water stress. State variables (Table 1) are updated using Euler integration with a one-day time step. The model is designed to simulate the entire plant, stalk and root biomass, sucrose concentration, plant phenology and other variables. It requires soil parameters that regulate the soil water balance (field capacity, wilting point, water saturation, and soil depth), daily weather variables (solar radiation, maximum and minimum temperatures, precipitation), and irrigation.

The model engine and modules are coded in FORTRAN 90 because it continues to be the predominant programming language of simulation modeling in agri-

§Present address: USP/ESALQ – Dept. Biosystems Engineering, Av. Pádua Dias, 11 – 13418-900 – Piracicaba, SP – Brasil.

Table 1 – Model state variables, descriptions, units and categories.

| State Variables | Description | Units | Category |
|---|---|---|---|
| NSTK | Number of stalks per area unit | stalk $m^{-2}$ | Phenology |
| LN | Number of green leaves per stalk | Leaves $stalk^{-1}$ | Leaf Development |
| LNTOTAL | Number of green plus dead leaves per stalk | Leaves $stalk^{-1}$ | Leaf Development |
| LA | Leaf area | $m^2$ | Leaf Development |
| W | total plant dry matter weight | t $ha^{-1}$ | Photosynthesis |
| WA | aerial dry matter weight | t $ha^{-1}$ | Biomass accumulation |
| WR | root dry matter weight | t $ha^{-1}$ | Biomass accumulation |
| WSDM | stalk dry matter weight | t $ha^{-1}$ | Biomass accumulation |
| WSFM | stalk fresh matter weight | t $ha^{-1}$ | Biomass accumulation |
| WL | leaf dry matter weight | t $ha^{-1}$ | Biomass accumulation |
| WSUC | Sucrose weight | t $ha^{-1}$ | Sucrose accumulation |
| SLENG | Stalk length | m | Plant extension |
| RLD | Root length density for L layer | cm $cm^{-3}$ | Root and water stress |
| $SWC_a$ | actual soil water storage in the profile | mm | Soil Water |

culture and due to the ease of obtaining available free code for specific algorithms used in this model.

**Crop components**

The model applies a similar approach to that used in the current Canegro model (Singels et al., 2008, included in Decision Support System for Agrotechnology Transfer - DSSAT) for the development of individual leaves and shoots and then scales up to a per-unit land area by multiplying the leaf area per shoot and the number of shoots per unit area. Tiller development is based on Inman-Bamber (1991), in which thermal time functions describe the tillering rate, maximum tiller population, and senescence. Each tiller is assumed to be a stalk at maturity, and all developmental variables are stalk based. Related parameters are CHUPEAK, CHUDEC, and CHUMAT (Table 2, Figure 1).

Leaf emergence is based on a simplification of the approaches used in APSIM-Sugar and DSSAT/CANEGRO, in which a unique phyllochron interval (PHY, Table 2) regulates the leaf emission rate. The canopy leaf area algorithm assumes leaves having area that is given by a mean leaf area (MLA, Figure 2), which in turn changes with plant phenology. When LN reaches Lfmax (Table 1), the older leaf is senesced, and its respective area is subtracted from total leaf areas. The daily leaf number increment (dNLeaf) is the product of daily accumulated growth degree-days (GDD) by PHY. The data used to adjust the optimization ranges of each of these parameters are given in Marin et al. (2011).

One difference compared to the approaches used both in APSIM-Sugar and DSSAT/CANEGRO is the assimilated constraint for leaf area, based on a source-sink approach for the carbon balance. The "sink" is the demand for assimilation by growing leaves, and the source is the supply of assimilates available for leaves on each day. When the carbohydrate amount needed for leaf biomass growth exceeds the available biomass for leaf growth, dNLeaf is reduced to fit the available leaf growth biomass, using a specific leaf area (SLA, Eq. 1). The values given by Eq. 1 compare well with Irvine (1975) and Silva et al. (2005). Although SLA may vary with cultivar and in response to other variables, we assumed a constant relationship (Eq. 1) between SLA and leaf number because of the lack of sufficient evidence on how other factors affect SLA. A desired further improvement on this issue would be to specify a maximum cultivar-specific SLA instead of the following distribution of SLA vs. LN, since more data are available for cultivars.

$$SLA = \begin{cases} = -0.0133 \cdot LN^2 + 0.3997 \cdot LN + 6.333 & \forall LN \leq 35 \\ = 4 & \forall LN > 35 \end{cases} \quad (1)$$

The model computes gross photosynthesis and respiration as used by CROPGRO (Boote et al., 1998) (Eq. 2, 3, and 4). This method was modified from the original version of the CASUPRO model (Villegas et al., 2005; Royce, 2010) in order to better simulate the photosynthetic rate response to $[CO_2]$ increase for a C4 species. The method uses the daily solar radiation absorbed by the leaf area of the cane to compute a daily rate of $CH_2O$ production. Radiation interception is calculated through Beer's law.

$$PG = PTSMAX * LI * AGEF * PRATIO * SWSP \quad (2)$$

$$PTSMAX = PHTMAX \cdot \left(1 - e^{\left(-\frac{PAR}{PARMAX}\right)}\right) \quad (3)$$

$$PRATIO = CCMAX \cdot \left(1 - e^{\left(-\frac{CCEFF}{CCMAX} \cdot co_2\right)}\right) \quad (4)$$

where PG is the daily rate of carbohydrate production (g $m^{-2}$ $d^{-1}$) [ground area basis]; AGEF is the age factor reducing the elongation as a plant becomes older (Eq. 5), representing the late decrease in stem elongation rate related to the lower specific leaf N content, which likely depresses the photosynthetic potential (Allison et al., 2007; Inman-Bamber et al., 2008); LI is the proportion of radiation interception able to be captured by the canopy, as a function of LAI and the extinction coefficient (EXTCOEF); PRATIO is the relative effect

Table 2 – Cultivar-specific parameters, descriptions, optimized values, range used for GLUE optimization, and units.

| Category | Parameter | Description | Optimized value | Range | | Units |
|---|---|---|---|---|---|---|
| | | | | MAX | MIN | |
| Photosynthesis | CCEFF | Relative efficiency of $CO_2$ assimilation used in equation to adjust canopy photosynthesis with $CO_2$ concentrations | 0.007[1] | * | * | dimensionless |
| | CCMAX | Max daily canopy photosynthesis relative to photosynthesis at $CO_2$ concentration 390 vpm | 1.09[1] | * | * | dimensionless |
| | PHTMAX | Maximum amount of $CH_2O$ which can be produced if PAR is very high | 282.9 | 200[1] | 284[1] | g[$CH_2O$] $m^{-2}$ $day^{-1}$ |
| | PARMAX | PAR at which photosynthesis is 63 % of the maximum value | 56.2 | 40[1] | 80[1] | moles[quanta] $m^{-2}$ $day^{-1}$ |
| | EXTCOE | Light extinction coefficient | 0.73 | 0.68[1] | 0.76[2] | dimensionless |
| Phenology | POP_PEAK | Maximum tiller population | 12 | * | * | stalks $m^{-2}$ |
| | POP_MAT | Stalk population at maturation | 8 | * | * | stalks $m^{-2}$ |
| | CHUDEC | Cumulative growing degree-days to start tiller decrease | 3150 | * | * | °C day |
| | CHUEM | Cumulative growing degree-days to emergence for a plant crop | 340 | 280 | 450 | °C day |
| | CHUMAT | Cumulative growing degree-days to stop tiller decrease and stabilize for maturation, after planting | 2850 | * | * | °C day |
| | CHUPEAK | Cumulative growing degree-days to peak tiller population, after planting | 1950 | * | * | °C day |
| | CHUSTK | Cumulative heat unit from emergence to start of stalk growth, after plant emergence | 450 | 400 | 600 | °C day |
| Leaf development | SLA | Specific leaf area in a fresh mass basis, assuming water content in leaves as 70 %. | (Eq.1) | * | * | g $m^{-2}$ |
| | $MLA_{max}$ | Maximum leaf area of a single leaf | 0.075 | * | * | $m^2$ |
| | $MLA_{end}$ | Leaf area of a single leaf at the end of the cycle | 0.055 | * | * | $m^2$ |
| | $LN_{peak}$ | Number of leaves to reach the maximum area of a single leaf | 22 | * | * | leaves |
| | $LN_{dec}$ | Number of leaves to begin the decrease of the area of a single leaf | 32 | * | * | leaves |
| | TBASE | Base temperature for photosynthesis and canopy development | 9.50 | 8[3] | 12[4] | °C |
| | PHY | Phyllocron interval | 122 | 69[2] | 169[2] | °C day |
| | LFMAX | Maximum number of green leaves a healthy, adequately-watered plant will have after it is old enough to lose some leaves | 9.5 | 6[5] | 135 | leaves |
| Biomass partitioning | MINRGPF | Minimum fraction of dry mass allocated to root mass | 0.09 | 0.08[6] | 0.14[6] | t $t^{-1}$ |
| | MAXLGPF | Maximum fraction of dry mass allocated to leaf mass | 0.45 | 0.40[6] | 0.46[6] | t $t^{-1}$ |
| Sucrose partitioning | SUCMAX | Maximum sucrose contents in the base of stalk in a dry mass basis | 0.65 | 0.49[7] | 0.75[6] | t $t^{-1}$ |
| Plant Extension | PERCOEF | Extension rate for unstressed plants | 0.29 | 0.176[8] | 0.352[8] | mm °C day |
| Root and Water Stress | RWEP1 | Soil water supply/potential evaporation ratio threshold below which photosynthesis is limited | 19 | * | * | dimensionless |
| | RWEP2 | Soil water supply/potential evaporation ratio threshold below which expansive growth is limited | 2[9] | * | * | dimensionless |
| | SRL | Specific root length | 13.6 | 5[10] | 18[10] | m $g^{-1}$ |

*The parameter was not optimized. [1]Modified after Royce et al. (2010) for atmospheric $CO_2$ concentration of 390 vpm; [2]Field measurements; [3]O'Callaghan et al. (1994); [4]Inman-Bamber (1994); [5]Nassif et al. (2012); [6]Marin et al. (2011); [7]Robertson et al. (1996); [8]Singels et al. (2008); [9]Jones & Kiniry (1986); [10]Laclau & Laclau (2009).

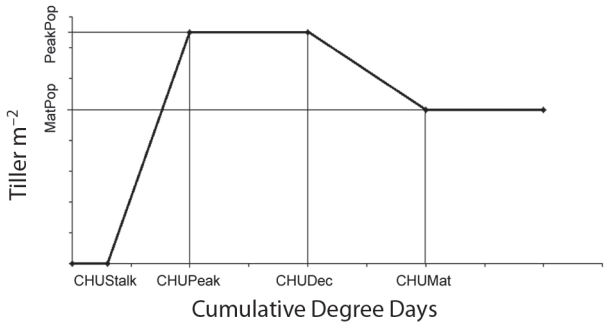


Figure 1 – Schematic representation of the tiller development algorithm used in the model.

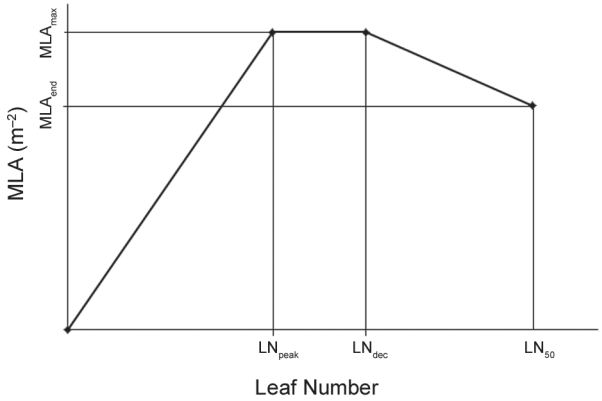


Figure 2 – Schematic representation of the leaf area module used in the model, where LN is the leaf number and MLA is the leaf area for a unique leaf.

of air $CO_2$ concentration ([$CO_2$]) on canopy PG, which corrects the computed PG using a standard value of 330 vpm.

For the simulations here we assumed [$CO_2$] = 330 vpm and therefore PRATIO = 1; PTSMAX is the potential amount of $CH_2O$ that can be produced at the specified PAR for full canopy (LAI > 8) when all other factors are optimal (g[$CH_2O$] $m^{-2}$ $d^{-1}$); SWSP is the effect of soil-water stress on photosynthesis (below described in Eq. 18), with SWSP = 1 meaning no stress, and SWSP = 0 meaning maximum stress. CCMAX and CCEFF are described in Table 2.

$$AGEF = e^{[-0.000401\cdot(DIAC-CHUSTALK)]} \quad (5)$$

where DIAC are the accumulated degree-days along the cycle, and CHUSTK is described in Table 2.

The daily respiration rate was computed with the approach developed by McCree (1974) using fitted coefficients for grain sorghum in Eq. 6.

$$RESP = 0.14 \cdot PG + CT \cdot W \quad (6)$$

$$CT = (0.044 + 0.0019 \cdot T_{mean} + 0.001 \cdot T^2_{mean}) \cdot 0.0108 \cdot W \quad (7)$$

where RESP is the daily respiration (g $m^{-2}$ $d^{-1}$) [ground area basis]; CT is a growth coefficient dependent on air temperature; $T_{avg}$ is the mean air temperature (°C); W is the total plant dry biomass (g $m^{-2}$ $d^{-1}$) [ground area basis].

Stalk elongation is a function of thermal time in an hourly time-step (Eq. 8) and the age factor (AGEF, Eq. 5) following Inman-Bamber et al. (2008):

$$dPER = (2.95 \cdot THour - 0.8516 \cdot PERCOEF \cdot SWSG \quad (8)$$

where dPER is the plant elongation rate (mm $h^{-1}$), and THour is the hourly temperature (°C). The hourly temperature was calculated using the synthetic temperature distribution proposed by Parton and Logan (1981). PERCOEF is the fraction of plant elongation due to stalk elongation (Table 2); and SWSG is the soil water stress factor for vegetative growth as shown in Eq. 19.

Partitioning for leaves, stalk and roots are described below and in equations 9 and 10. When the leaf growth partitioning factor (LGPF) is larger than the maximum LGPF (MAXLGPF), the difference (LGPF-MAXLGPF) is added to the stalk growth partitioning factor (SGPF). Stalk and root partitioning (RGPF) is regulated by the sink capacity for stalk structural growth. For DIAC < CHUEM it was assumed RGPF = 1, SGPF = 0.0, and LGPF = 0. For CHUEM < DIAC < CHUSTK, it was assumed SGPF = 0.0, RGPF was calculated with Eq. 9 and LDPF as the complementary value. Finally, when DIAC > CHUSTK, the model first allocates the carbohydrate to the roots with Eq. (9) (never less than MINRGPF), assumes LGPF = MAXLGPF, and then calculates the amount derived for stalks using Eq. (10). In the cases SGPF + RGPF + LGPF > 1, a restriction is imposed on the SGPF to match the unit.

$$RGPF = \frac{1-\text{MAXLGPF}}{1+e^{DIAC\cdot\left(\frac{6}{CHUSTK}-6\right)}} + \text{MINRGPF} \quad (9)$$

$$SGPF = \frac{1-\text{RGPF}-\text{LGPF}}{1+\text{CHUSTK}\cdot e^{-DIAC}} \quad (10)$$

where LGPF is the leaf growth partitioning factor, RGPF is the root growth partitioning factor, and SGPF is the stalk growth partitioning factor. MAXLGPF, MINRGPF and CHUSTK are described in Table 2.

Differently from other sugarcane models, sucrose accumulation is calculated in an internode basis. The partitioning of stalk dry mass between stalk structure and sucrose is regulated by sink capacity, the thermal age of the internode, and characteristics of the cultivar. Sucrose partitioning is considered the fourth priority after leaves, roots and stalk fiber. The framework describing the sucrose accumulation was based on Uys et al. (2007) and empirically derived from the data of van Dillewijn (1952). The approach relies on the concept that exceeding photosynthates are driven to sucrose; despite the simplification embedded in this approach (Alexander, 1973), it is still a useful tool to account for sucrose accumulation.

Partitioning factors for sucrose (SUCPF, Eq. 11) and fiber (FIBPF, Eq. 12) and updated daily for each internode (IN). The effect of temperature on sucrose accumulation is indirectly accounted for by the leaf, root and stalk growth rate responses to temperature because low temperatures reduce growth rate before photosynthesis, making more photosynthates available for sucrose accumulation. In addition, water deficit is indirectly accounted for by its differential effect on expansive growth and photosynthesis. Expansive growth is reduced faster than photosynthesis, accelerating the process of sucrose accumulation under conditions of middle water deficits and lower temperatures.

$$SUCPF_{IN} = \frac{SUCMAX}{[1+EXP(-IN+6)]} \quad (11)$$

$$FIBPF_{IN} = 1 - SUCPF_{IN} \quad (12)$$

where SUCMAX is the maximum sucrose content in the internode (t $t^{-1}$); IN is the internode number starting with the first internode at the basis of the stalk.

Root growth was expressed in terms of the extent of the rooting depth and root length in each soil layer. The rate of deepening of the root front was based on Laclau and Laclau (2009) (0.03 cm $°C^{-1}$ $day^{-1}$). The soil water balance requires the input of a root weighting factor ($RWF_i$), a relative variable ranging from 1 – a soil most hospitable to root growth – to near 0 – soil inhospitable to roots (Ritchie 1998), for each soil layer (*i*) (Eq. 13). The sum of all $RWF_i$ for the entire profile should be equal to 1. Because the distribution of sugarcane root length

is similar to an exponential pattern (Liu and Bull, 2001; Laclau and Laclau, 2009), RWF values were estimated using the approach proposed by Jones et al. (1991) using an exponential geotropism constant equal to 2.

$$RWF_i = \frac{\frac{(1-L_i)}{S_{maxdepth}}}{\sum_{i=1}^{n}\frac{(1-L_i)}{S_{maxdepth}}} \quad (13)$$

where $L_i$ is the soil layer depth $i$, $S_{maxdepth}$ is the maximum root depth in the soil profile assumed in the simulations, and $n$ is the number of soil layers.

Root senescence is assessed by Eq. 14, derived from the results of Jones & Kiniry (1998) and Ball-Coelho et al. (1992).

$$RootSene = \frac{(0.15 \cdot WR)}{(WR+1)} \quad (14)$$

where RootSene is the percentage of total root senesced each day, and WR is the total root dry mass (g $m^{-2}$) [ground basis].

Root water absorption follows Ritchie (1998) by assuming the water movement into a single root, that the roots are uniformly distributed within a layer, and that the maximum daily root water uptake equals 0.07 $cm^3$ $day^{-1}$ (Singels et al., 2008). The potential root water uptake ($RWU_i$) as influenced by soil water flow to roots in a layer is calculated by Eq. 15 and integrated for the whole soil layer $RWUL_i$ using Eq. 13 as in Jones and Kiniry (1986). Total root water uptake from the entire root zone (TRWU) is obtained by the integration of $RWUL_i$ for the entire profile.

$$RWU_i = \frac{0.00267 \cdot \exp(62 \cdot (\theta_{v(i,t)} - \theta_{v(i,LL)})}{(6.68 - \ln(RLD_i))} \quad (15)$$

$$RWUL_i = RWU_i \cdot L_i \cdot RLD_i \quad (16)$$

where $RWU_i$ is the potential root water uptake ($cm^3$[water] cm[root]$^{-1}$ $d^{-1}$); $RWUL$ is the potential root water uptake ($cm^3$ [water] $d^{-1}$); $L_i$ is the layer length (cm); and $RLD_i$ is the root length density in the soil layer ($i$) cm [root] $cm^{-3}$ [soil].

$RLD_i$ is calculated following Jones & Kiniry (1986) by using Eq. 17 and a factor given by a water uptake fraction (WUF) to reduce the potential water uptake as given by the ratio between EPp and TRWU:

$$RLD_i = (W_r \cdot SLR \cdot RWF_i) \cdot R_{depth}^{-1} \quad (17)$$

where Wr is the root dry matter weight (g $cm^{-2}$); SLR is the specific root length (g $cm^{-1}$); RWF is the root weighting factor (unitless) for the layer ($i$); and $R_{depth}$ is the root depth (cm).

Two soil water deficit factors are calculated to account for water stress on biomass production (SWSP) and expansive growth (SWSG), as used in DSSAT/CANEGRO. Both are calculated from the ratio of the potential uptake to the potential transpiration (Ritchie, 1998). SWSP and SWSG are assumed to be reduced linearly from 1.0 to 0.0 when the potential uptake to the potential transpiration ratio falls below 1.0 and 2.0, respectively (Jones and Kiniry, 1986). Any stress due to nutritional restrictions was not simulated.

Soil water stresses are computed in two ways (Jones and Kiniry, 1986). The first computes the effect of water deficit on photosynthesis and biomass production (SWSP, Eq. 18) and the second (SWSG, Eq. 19) computes the effects of water deficit on more sensitive plant physiological process, such as tillering, stalk elongation, and leaf expansion.

$$\text{SWSP} = \text{MIN}\left(1., \left(\frac{\text{EPp}}{RWUEP_1 \cdot \text{TRWU}}\right)\right) \quad (18)$$

$$\text{SWSG} = \text{MIN}\left(1., \left(\frac{\text{EPp}}{RWUEP_2 \cdot \text{TRWU}}\right)\right) \quad (19)$$

where RWUEP1 is the soil water supply/potential evaporation ratio threshold below which evaporation and photosynthesis are reduced, set as 1 and RWUEP2 is the soil water supply/potential evaporation ratio threshold below which expansive growth is limited, set as 2 following the concepts embodied in the CERES models (Jones and Kiniry, 1986).

**Soil components**

For simplicity, the soil-water balance was designed for a four-layer soil following the classic approach based on Darcy and Buckingham´s (1907) law and subsequently summarized by Teh (2006), in which the volumetric water content in a soil layer (i) at time (t) is given by Eq. 20:

$$\theta_{v(i,t)} = \theta_{v,sat} - \frac{\theta_{v,sat}}{\alpha} ln\left\{\frac{\alpha K_{sat} \Delta t}{L_i \theta_{v,sat}} + exp\left[\frac{\alpha}{\theta_{v,sat}}\left(\theta_{v,sat} - \theta_{v(i,t-1)}\right)\right]\right\} \quad (20)$$

where $\theta_{v(i,t)}$ is the current and volumetric water content ($m^3$ $m^{-3}$) and $\theta_{v(i,t-1)}$ is the last calculated volumetric water content ($m^3$ $m^{-3}$) in the soil profile (i); $L_i$ is the thickness (m) of soil layer $I$; $\Delta t$ is the time step (day); $\alpha$ was set as 13 assuming an homogeneous soil (Reichardt et al., 1972); and $\theta_{v,sat}$ is the volumetric water at saturation ($m^3$ $m^{-3}$). The water uptake by roots or evaporation is included in the equation by the subtraction of the water used by the plant and evaporated in the previous day from $\theta_{v(i,t-1)}$.

Hydraulic conductivity was assumed to be related to soil wetness by an exponential relationship (Kendy et al., 2003) (Eq. 21):

$$K_{(\theta)} = K_{sat} \cdot exp\left[-\alpha \frac{(\theta_{v,sat} - \theta_{v(i,t)})}{(\theta_{v,sat} - \theta_{v,r})}\right] \quad (21)$$

where Ksat is the saturated hydraulic conductivity (m $day^{-1}$); $\alpha$ is an empirical coefficient (dimensionless); and $\theta_{v,sat}$ and $\theta_{v,r}$ are the saturated and residual volumetric soil water contents ($m^3$ $m^{-3}$), respectively. $\theta_{v,r}$ was set as zero.

The equations to predict evapotranspiration (ETp) from soil and plant surfaces are those described by Ritchie (1998), but the Penman equation (Penman, 1948) is re-

placed by the Priestley and Taylor (1972) method because of the lack of data on vapor pressure and wind for the studied locations. The calculation of evapotranspiration with a modified Priestley-Taylor equation is fully described in Ritchie (1998). An algorithm for computing Penman-Monteith evapotranspiration (Allen et al., 1998) might be used for locations for which input data are available.

Calculation of potential evaporation with a modified Priestley-Taylor equation (Eq. 22) requires an approximation of daytime temperature (TD) (Eq. 23) and a soil plant reflection coefficient (ALB) (Eq. 24) for solar radiation.

$$ETp = f \cdot [SRAD \cdot (0.00488 - 0.00437 \cdot ALB \cdot (TD + 29)] \quad (22)$$

$$TD = 0.6 \cdot T_{max} + 0.4 \cdot T_{mim} \quad (23)$$

$$ALB = 0.1 \cdot e^{(-0.7 \cdot LAI)} + 0.2 \cdot (1 - e^{(-0.7 \cdot LAI)}) \quad (24)$$

where Tmax and Tmin are, respectively, maximum and minimum air temperature (°C); f is the air temperature related correction factor, given by Eq. 25. Prior the germination, ALB is assumed to be the bare soil albedo.

$$f = \begin{cases} 0.01 \cdot e^{0.18 \cdot (Tmax + 20)} & \forall \quad Tmax < 5°C \\ 1.1 + 0.05 \cdot (Tmax - 35) & \forall \quad Tmax > 35°C \\ 1.1 & \forall\ 5°C \leq Tmax \leq 35°C \end{cases} \quad (25)$$

Evapotranspiration partitioning in transpiration (EPp) and evaporation (ESp) is represented in Eqs. 26 and 27. Potential soil evaporation is scaled down to actual evaporation by a reduction factor ($R_{d,e}$), which is calculated using the relative water content, defined by the ratio between the current volumetric water content and the water content at saturation (Keulen and Seligman, 1987) (Eq. 28). For the period before plant emergence, the soil water balance is simulated considering only soil evaporation and deep drainage as soil water drains.

$$ESp = ETp \cdot e^{-0.7 \cdot LAI} \quad (26)$$

$$EPp = ETp \cdot [1 - e^{-0.7 \cdot LAI}] \quad (27)$$

$$R_{d,e} = \frac{1}{1 + \left[3.6073 \cdot \left(\frac{\theta_v}{\theta_{v,sat}}\right)\right]^{-9.3172}} \quad (28)$$

## Data sources

### Crop data

The model was parameterized and evaluated using plant cane and first ratoon data from the SP83-2847 cultivar, collected in four locations in Southern Brazil. The experimental data were provided by Suguitani (2006), Laclau and Laclau (2009), Tasso (2007), and Santos (2008), as described in Table 3, and the variables collected and measurement frequency are fully described in Marin et al. (2011) (Table 3). All experiments received adequate N, P and K fertilization and regular weed control and were planted using healthy cuttings with 13 to 15 buds $m^{-2}$. Row spacing varied from 1.4 m to 1.5 m. One of the datasets had two treatments (irrigated and rainfed), and all the remaining experiments were rainfed. The irrigated treatment received water by sprinkling, and matric potential was measured with tensiometers to maintain the soil layers close to field capacity, down to a depth of at least 1 m.

SP83-2847 was among the five most commonly grown cultivars in Southern Brazil in 2011. It is late maturing, with high cane and sucrose yields when grown either as a plant crop or ratoon.

### Soil Data

As soil water parameters were not measured, the values of volumetric water at saturation ( $\theta_{v,sat}$, $m^3$ $m^{-3}$), volumetric water at soil water lower limit for the crop ($\theta_{v,ll}$, $m^3$ $m^{-3}$), and the volumetric water at soil water drained upper limit ($\theta_{v,ul}$, $m^3$ $m^{-3}$) were defined using the pedotransfer functions (PTF) provided by Tomasella et al. (2000) (Table 4). The hydraulic conductivity at saturation (KSat) was estimated based on Poulsen et al. (1999) as a function of saturated volumetric soil water content ($m^3$ $m^{-3}$) and drained soil porosity (Table 4). The input data for PTF (clay, sand, and organic carbon content, as well as soil bulk density) were measured in the respective experimental sites and provided by Suguitani (2005), Laclau and Laclau (2009), Tasso Jr. (2006) and Santos (2008).

### Parameter Estimation

The generalized likelihood uncertainty estimate (GLUE) (Beven and Binley, 1992; Franks et al., 1998; Shulz et al., 1999) method was used for the crop model optimization to determine the best set of parameters from such a number of samples. The GLUE method is a

Table 3 – Overview of experimental data from cultivar SP83-2847, soil and climate characteristics of each experiment site.

| Dataset | Site | Planting and Harvest Dates | Crop Cycle[1] | Climate[2] | Treatments |
|---|---|---|---|---|---|
| 1 | Piracicaba/SP, 22º52' S, 47°30' W, 560 m asml | 29 Oct 2004 and 26 Sept 2005 | PC | 21.6 °C, 1230 mm, CWa | 1) Irrigated, 2) Rainfed |
| 2 | Aparecida do Taboado/MS, 20º05'19" S, 51°17'59" W, 335 m asml | 1 July 2006 and 8 Aug 2007 | R1 | 23.5 °C, 1560, Aw | 3) Rainfed |
| 3 | Colina/SP, 20°25' S, 48°19' W, 590 m asml | 10 Feb 2004 and 15 June 2005 | PC | 22.8 °C, 1363 mm, Aw | 4) Rainfed |
| 4 | Olimpia/SP, 20°26' S, 48°32' W, 500 m asml | 10 Feb 2004 and 15 June 2005 | PC | 23.3 °C, 1349 mm, Aw | 5) Rainfed |

[1]PC - Plant cane crop; R - ratoon crop and following number is the ratoon rank; [2]Respectively: mean annual temperature, annual total rainfall, Koeppen Classification.

Table 4 – Soil properties input for the model for each dataset.

| Layer Depth | Lower limit | Upper limit drain. | Upper limit sat. | Sat. hyd. cond. |
|---|---|---|---|---|
| | cm cm$^{-3}$ | | | cm h$^{-1}$ |
| Dataset 1 – Latossolo Vermelho-Amarelo (Typic Hapludox)* | | | | |
| 20 | 0.200 | 0.310 | 0.480 | 0.380 |
| 40 | 0.225 | 0.330 | 0.480 | 0.390 |
| 100 | 0.238 | 0.338 | 0.485 | 0.400 |
| 450 | 0.250 | 0.350 | 0.490 | 0.360 |
| Dataset 2 – Latossolo Vermelho-Amarelo (Typic Hapludox)* | | | | |
| 20 | 0.140 | 0.180 | 0.430 | 4.390 |
| 40 | 0.135 | 0.205 | 0.390 | 4.385 |
| 100 | 0.140 | 0.203 | 0.400 | 4.373 |
| 180 | 0.150 | 0.190 | 0.410 | 4.370 |
| Dataset 3 – Latossolo Vermelho-Escuro (Typic Hapludox)* | | | | |
| 20 | 0.115 | 0.210 | 0.440 | 0.850 |
| 40 | 0.120 | 0.220 | 0.440 | 0.745 |
| 100 | 0.120 | 0.210 | 0.420 | 0.715 |
| 350 | 0.120 | 0.210 | 0.420 | 0.700 |
| Dataset 4 – Latossolo Vermelho-Escuro (Typic Hapludox)* | | | | |
| 20 | 0.165 | 0.370 | 0.480 | 1.32 |
| 40 | 0.160 | 0.370 | 0.480 | 1.25 |
| 100 | 0.160 | 0.370 | 0.440 | 1.22 |
| 350 | 0.160 | 0.370 | 0.440 | 1.22 |

*Soil Classification by Brazilian Soil Classification System and their nearest US Soil Taxonomy equivalent (in brackets).

Bayesian method that assumes that in large models with many parameters, there is no exact inverse solution. Hence, the estimation of a unique set of parameters that optimizes a goodness-of-fit criterion given the observations is not possible (Romanowicz and Beven, 2006). Based on He et al. (2012), we assumed that the parameters followed normal distributions.

Many parameter sets are generated from specified prior distributions of parameters and then used to simulate outputs by Monte Carlo simulation. We generated N multivariate normal realizations of parameter sets with each set containing the following parameters in Table 1: PHTMAX, PARMAX, EXTCOEF, CHUEM, CHUSTK, TBASE, PHY, LFMAX, MINRGPF, MAXLGPF, SUCMAX, PERCOEF, and SRL. From the point of view of Monte Carlo sampling in the GLUE method, more parameter sets lead to more stable results (He et al., 2010), and here, we used 6000 samples that were considered to be independent. The performance of each parameter set in predicting observed model states is evaluated via a likelihood measure that is used to weight the predictions from the parameter sets (He et al., 2010). The GLUE method transforms the problem of searching for an optimum parameter set into a search for sets of parameter values that would give reliable simulations for a range of model inputs (Candela et al., 2005).

The main principle of this method is to discretize the parameter space, by generating a large number of parameter values from the prior distribution (Jones et al., 2011). Different sets of initial boundary conditions or model structures can also be considered. Based on comparing predicted and observed responses, to each set of parameters values is assigned a likelihood of being a simulator of the system. The definition of the likelihood measure is intrinsic to the GLUE framework, and the uncertainty prediction can strongly depend on that definition (Ratto et al., 2010). In a Bayesian framework, this definition is connected to how errors in the observations and in the model structure are represented by a statistical model. Different possible likelihood functions can be selected. We used Eq. 29 as a likelihood function following He et al. (2009), who found that it produced model outputs from the posterior distribution that were closest to the field observations.

$$L(S_i|O) = \prod_{i=1}^{M} \frac{1}{\sqrt{\pi \cdot 2 \cdot \sigma_o^2}} \cdot e^{\left[ \frac{\left[O_j - P(S_i)\right]^2}{2 \cdot \sigma_o^2} \right]} \quad (i = 1,2,3,\ldots N) \qquad (29)$$

where $S_i$ is $i$th parameter set; $P_j(S_i)$ the $j$th type of model output under parameter set $\theta_I$; O is the observation; $O_j$ the $j$th observation of O; $\sigma_o^2$.the variance of model errors, assumed to be the variances of observations in this study; N the number of random parameter sets; and M the number of replicates of the observations.

Using Eq. 30, we rescaled the likelihood measures such that the sum of all the likelihood values equals 1 yielding a distribution function for the parameters sets. Likelihood values were then calculated for each parameter set using field observations. Sucrose and fresh stalk mass, tillering, and leaf area index data were considered the observed variables.

$$L(S_i) = \frac{L(S_i|O)}{\sum_{i=1}^{N} L(S_i|O)} \qquad (30)$$

where $L(S_i)$ is the likelihood weight of the $i$th parameter set $\theta_i$; $L(S_i|O)$ is the likelihood value of parameter set $S_i$, given the observation O.

**Model Evaluation**

Considering that different sets of observations were taken in each dataset at different frequencies, we chose the leave-one-out cross-validation method of data splitting (Wallach et al., 2006) to simultaneously include all the variability in conditions and measurements in the parameter estimation and model predictions evaluation. The leave-one-out cross-validation procedure had a factorial design in which each run missed one treatment each time. So, five simulation combinations were carried out for cultivar SP83-2847. The parameter set (PHTMAX, PARMAX, EXTCOEF, CHUEM, CHUSTK, TBASE, PHY, LFMAX, MINRGPF, MAXLGPF, SUCMAX, PERCOEF, and SRL) was shown as the final optimized parameters for the cultivar.

A major decision about which parameters to optimize was based on available measured data, to avoid adjusting parameters that were not related to available data. To determine which parameters to estimate, a targeted

sensitivity analysis was first performed to determine the dependency of simulated variables on changes in key parameters. Parameters for which variation ranges could not be found in the literature or that are well known or easily measured did not form part of optimization routine.

Means were compared against the independent experimental data collected using five datasets (Table 2) and using the following outputs: LAI, stalk and aerial dry mass, number of green leaves and stalk height, and sucrose mass. Details in measurements and frequencies are in Marin et al. (2011), and these treatments were chosen for the evaluation procedure because they were obtained from better-detailed experiments, with higher frequencies of measurement. The quality of the predictions was computed using bias, root mean squared error (RMSEP), modeling efficiency (Eff) (Wallach et al., 2006), correlation coefficient, and agreement index (Willmott, 1981) as agreement measures.

## Results and Discussion

### Parameter Estimation

The values obtained using GLUE in addition to the cross validation technique are summarized in Table 5. LFMAX and SUCMAX are parameters conceptually derived from DSSAT/CANEGRO, what we have compared to those suggested for DSSAT/CANEGRO's standard cultivar NCo376. Values of SUCMAX were slightly higher than the values for NCo376, but were still within the range proposed by Singels and Bezuidenhout (2002) and Robertson et al. (1996). LFMAX ranged from 9 to 10 for all datasets. Thus, the optimized value (LFMAX = 9.5) expressed well the actual field observations for SP83-2847.

The parameters MAXLGPF and MINRGPF are difficult to evaluate, as we did not find other models using the same concept in the literature, nor measurements that would be comparable. Field data for SP83-2847 analyzed for partitioning studies in Brazil revealed leaf to above-ground biomass ratios ranging from 0.11 to 0.21. The ratio of stalk to above-ground biomass ranged from 0.46 to 0.66 (Figure 3). The leaf to above-ground biomass ratio decreased during the crop cycle from 0.21 to 0.11 kg $kg^{-1}$ for SP83-2847, regardless of the locations and the water application. From the leaf and stalk to above-ground biomass ratios, we can infer that roots received at least 13 % of the above-ground biomass. Laclau and Laclau (2009) reported root to total biomass ratios ranging from 0.61 to 0.09 for cultivar SP83-2847, which is comparable to 0.42 kg $kg^{-1}$ at 50 days of age as reported by Smith et al. (2005), and to 0.09 kg $kg^{-1}$ at harvest.

Table 5 – Optimized parameters values using five datasets for cultivar SP83-2847.

| Parameter | Optimized Value | Units |
|---|---|---|
| PHTMAX | 249.7 | g[$CH_2O$] $m^{-2}$ $day^{-1}$ |
| PARMAX | 56.4 | moles[quanta] $m^{-2}$ $day^{-1}$ |
| EXTCOE | 0.73 | dimensionless |
| CHUEM | 350.6 | °C day |
| CHUSTALK | 422.8 | °C day |
| LFMAX | 9.5 | leaves |
| MAXLGPF | 0.43 | t $t^{-1}$ |
| MINRGPF | 0.096 | t $t^{-1}$ |
| PHY | 121.7 | °C day |
| SUCMAX | 0.65 | t $t^{-1}$ |
| TBASE | 9.4 | °C |
| PERCOEF | 0.29 | mm °C day |
| SRL | 13.6 | m $g^{-1}$ |

The tillering pattern is similar to that described by Bezuidenhout et al. (2003), at 12 and 14 tiller $m^{-2}$ in the tillering peak (PEAKPop); after the senescence phase (POPMat), tiller density stabilized at 7 tiller $m^{-2}$. Stalk growth began at 772 °C day (CHUSTK) after planting, with peak tillering at 1950 °C day after planting.

PEAKPop and POPMat represent nearly half of the values found for the NCo376 cultivar. The lower tillering rate and number of final tillers observed in Brazilian fields seem to be related to their more rapid initial development and greater leaf area causing higher levels of light interception and early shadowing of the stalk base. This implies in the fact that the tillering rate is related to canopy light interception (van Dillewijn, 1952; Bezuidenhout et al., 2003) and is not simply a fixed response to temperature as calculated by the model. However, including algorithms to better describe the process inside the model, such as proposed by Bezuidenhout et al. (2003), implies in the need for the rate of bud emergence as input data, an issue rarely available for sugarcane.

The optimized value (121.8 °C day) for leaf phyllochron (PHY) compared well to the observed values in datasets 1 and 2 (Figure 4a), as well as to the literature (Singels et al., 2008; Sinclair et al., 2004). To calculate the leaf area an embedded algorithm was derived from the relationship obtained for SP83-2847 based on measurements of datasets 1 and 2 (Figure 4b). It considers a qua-

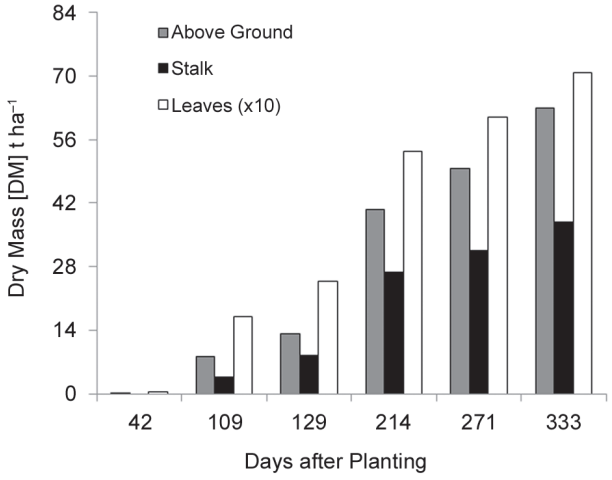


Figure 3 – Time series of root, stalk, above ground and green leaves dry mass for cultivar SP83-2847 in Piracicaba, SP, Brazil.

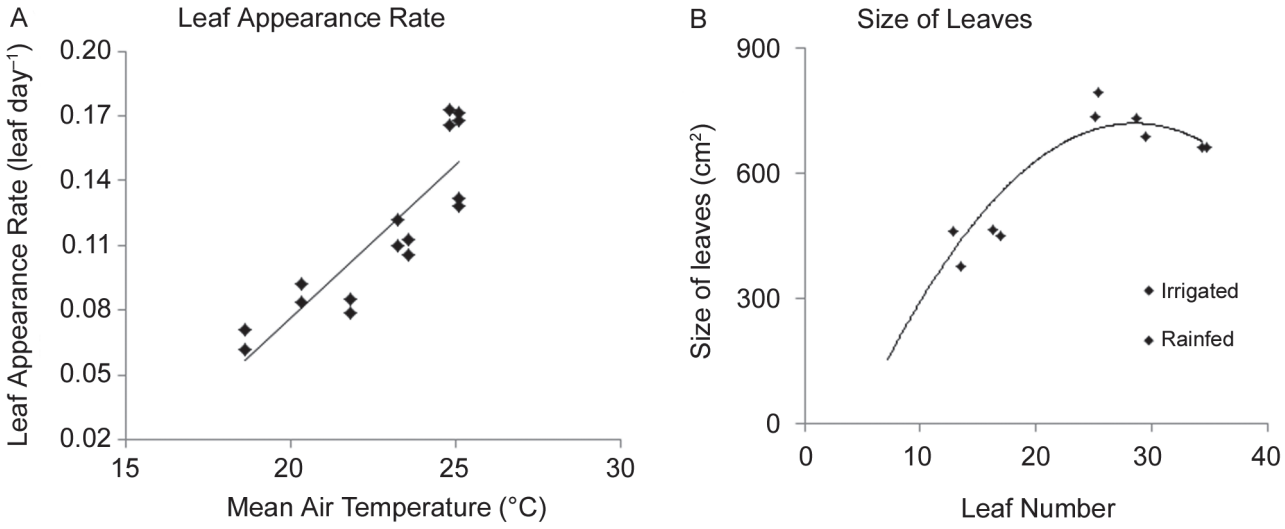


Figure 4 – A) Leaf development rate versus temperature; and B) leaf size and number of leaves relationship of cultivar SP83-2847.

dratic function for leaf area, simulation indistinctly for cultivars and is still an issue for further model improvement. The values obtained for SP83-2847, as large as 733 $cm^2$, represented nearly double the leaf area found for NCo376 in South Africa (Singels et al., 2008), but these values seem to be consistent with a range of Brazilian genotypes (Nassif et al., 2012).

The optimized value for specific root length (SRL) was 13.6 m $g^{-1}$. In spite of the lack of root data for SP83-2847, we consider this value very reasonable. Laclau and Laclau (2009), for instance, studied the root development of cultivar RB72-454 in the same environment in which treatments 1 and 2 were carried out and found SRLs ranging from 16 to 18 m $g^{-1}$ and 19 to 22 m $g^{-1}$, on average, from 125 DAP onwards in the rainfed and irrigated treatments, respectively. Mean SRL down to a depth of 1 m was 17.6 m $g^{-1}$ for rainfed and 19.1 m $g^{-1}$ for irrigated crops. Chopart et al. (1998) found a large range of SRLs (from 7 m $g^{-1}$ to 91 m $g^{-1}$) measured at 45 and 113 DAP down to a depth of 1.1 m in the Ivory Coast. Ball-Coelho et al. (1992) found SRLs near 16.5 m $g^{-1}$ in northeastern Brazil for the plant and first ratoon crop cycles.

The light extinction coefficient was optimized at 0.736, a value near to that determined based on canopy structure measurements for Brazilian cultivars using the approach developed by Campbell (1990). Royce (2010) suggested 0.80 for Floridian cultivars, as parameterized for the CASUPRO model.

Liu et al. (1998) reviewed several papers reporting base temperature values for sugarcane and found those estimates varied considerably. For example, O'Callaghan et al. (1994) used a base temperature of 8 °C for all stages of development, and Barnes (1964) estimated base temperature of 12 °C for germination. Inman-Bamber (1994) used base temperatures of 10 °C and 16 °C for leaf and tiller appearance, respectively. Bacchi and Sousa (1977) derived a base temperature of 18 °C for stalk elongation for Brazilian cultivars.

Based on this, it appears that the optimized Tb value for the model should better explain the leaf and tiller rates but may be below the reported values for stalk elongation. This result may be the reason for finding that PERCOEF was almost double the value used by Singels et al. (2008) in the DSSAT/CANEGRO. Based on this observation, it would be desirable to let Tb be free to vary during the optimization process in association with thermal time-related parameters, thus allowing the optimization to find the best answer to accommodate the parameters to the data.

## Model evaluation

### Leaf area and tillering

The parameterization used for the tillering algorithm described the five datasets reasonably well, resulting in RMSEP = 1.84 tiller $m^{-2}$ and Eff = 0.49. It was interesting to note the differences regarding tillering observed in the experimental fields of Colina (20°25′ S, 48°19′ W, 590 m asml) (Figure 5d), Olímpia (20°26′ S, 48°32′ W, 500 m asml) (Figura 5e) and Piracicaba (22°52′ S, 47°30′ W, 560 m asml) (Figures 5a, b) compared to Aparecida do Taboado (20°05′ S, 51°18′ W, 335 m asml) (Figure 5c). Considering the sites had similar soils (Table 4), the same cultivar, and minor air temperature differences (Table 3), the observed tillering pattern differences seem to be related to the germination rate and the number of effectively established plants, which were variables not measured. A previous attempt to improve the tillering algorithm using a mechanistic procedure (Bezuindeholt et al., 2003) was also abandoned due to the lack of such information and it should be considered in future efforts to improve this algorithm.

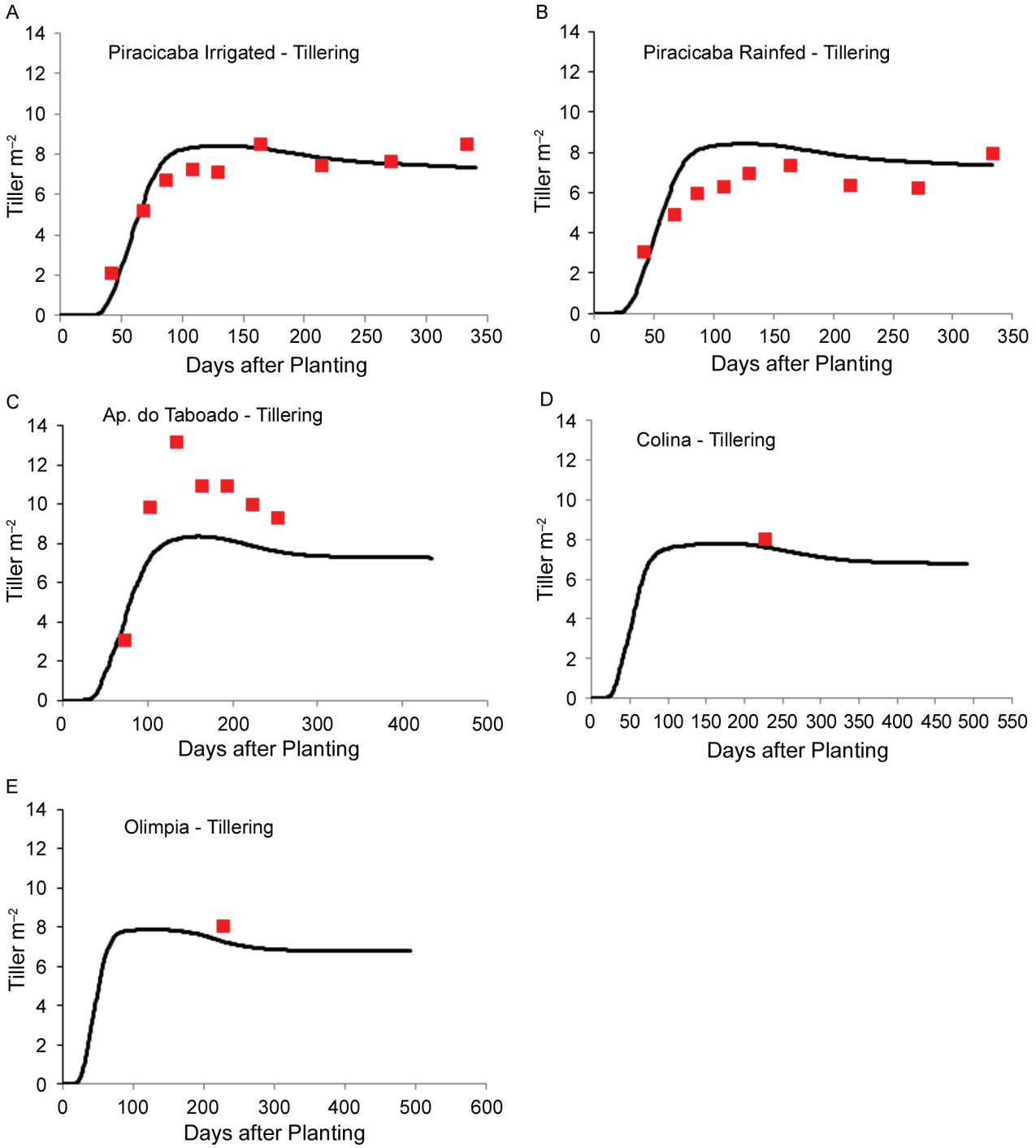


Figure 5 – Observed and simulated tillering (tiller $m^{-2}$) for five experiments for cultivar SP83-2847.

LAI was measured in only two experiments, and the algorithm used resulted in reasonable simulated values for green LAI (RMSEP = 0.89; Eff = 0.67). These results may be considered acceptable considering the experimental variability used in this calibration, but further algorithm improvement should take into account the possibility of adjusting the canopy leaf area as a function of the genotype. Figure 6 shows the limitations of the approach, primarily for the rainfed treatment, which possibly suggests the need for further studies related to the effect of water stress on canopy development.

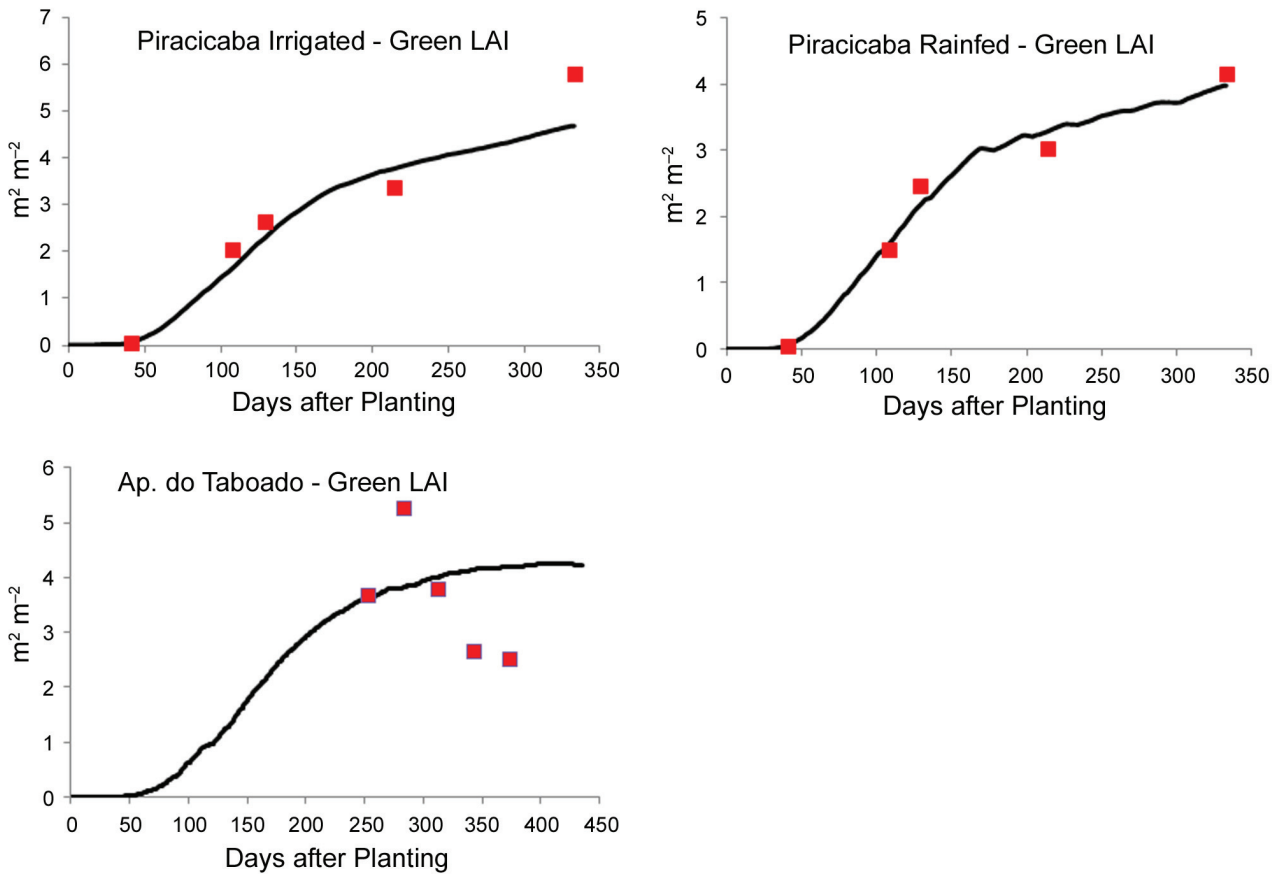


Figure 6 – Observed and simulated green leaf area index (Green LAI) for three experiments for cultivar SP83-2847, using optimized parameters from Table 2.

**Sucrose and Stalk Yield**

Because the model is intended to simulate partitioning among plant components, including stalk dry mass and sucrose, comparison of model predictions to these two frequently-available field measurements is particularly important. The RMSEP of 5.38 t ha$^{-1}$ for SP83-2847 (Table 6) is slightly lower than either of the values obtained by Singels and Bezuidenhout (2002), or O'Leary (2000) and Marin et al. (2011) using several versions of CANEGRO for simulations or values from Cheeroo-Nayamuth et al. (2000) using the APSIM-Sugar model to simulate sugarcane growth in Mauritius (RMSEP = 6.0 t ha$^{-1}$). Simulated stalk dry mass compared well with observed data (Figure 7), with the best agreement measures for the tested variables. Modeling efficiency reached 0.85 and the d-index was 0.98. An exception was for the experiment in Aparecida do Taboado (Figure 7c), where the model simulation overestimated the stalk dry mass, possibly because water stress effects were not captured adequately.

Agreement measures for sucrose content (POL) had lower predictive skills relative to the other variables, with Eff = 0.51 (Table 6, Figure 8). Results presented by Singels et al. (2008) for experiments in South Africa showed a similar trend to that observed here, overestimating sucrose content primarily in the early phase of the cycle.

Table 6 – Agreement measures of cross-validated predictions for cultivar SP83-2847, for stalk dry mass (STKH), sucrose content (SUCH), leaf area index (LAI), and tiller number per square meter (TILLER).

| Measure of Agreement | STKH | SUCH | LAI | Tiller |
|---|---|---|---|---|
| | t ha$^{-1}$ | % | | tiller m$^{-2}$ |
| Mean Obs. | 26.34 | 14.09 | 2.84 | 7.33 |
| St. dev. Obs. | 13.47 | 1.81 | 1.62 | 2.49 |
| Mean Sim. | 29.48 | 14.69 | 2.81 | 7.18 |
| St. dev Sim. | 14.94 | 1.45 | 1.43 | 1.83 |
| RMSEP | 5.38 | 1.17 | 0.85 | 1.73 |
| Mod Eff. | 0.84 | 0.57 | 0.70 | 0.50 |
| r | 0.95 | 0.82 | 0.84 | 0.71 |
| d-index | 0.96 | 0.87 | 0.91 | 0.81 |
| Bias | 3.14 | 0.59 | -0.03 | -0.15 |
| n | 15 | 27 | 15 | 27 |

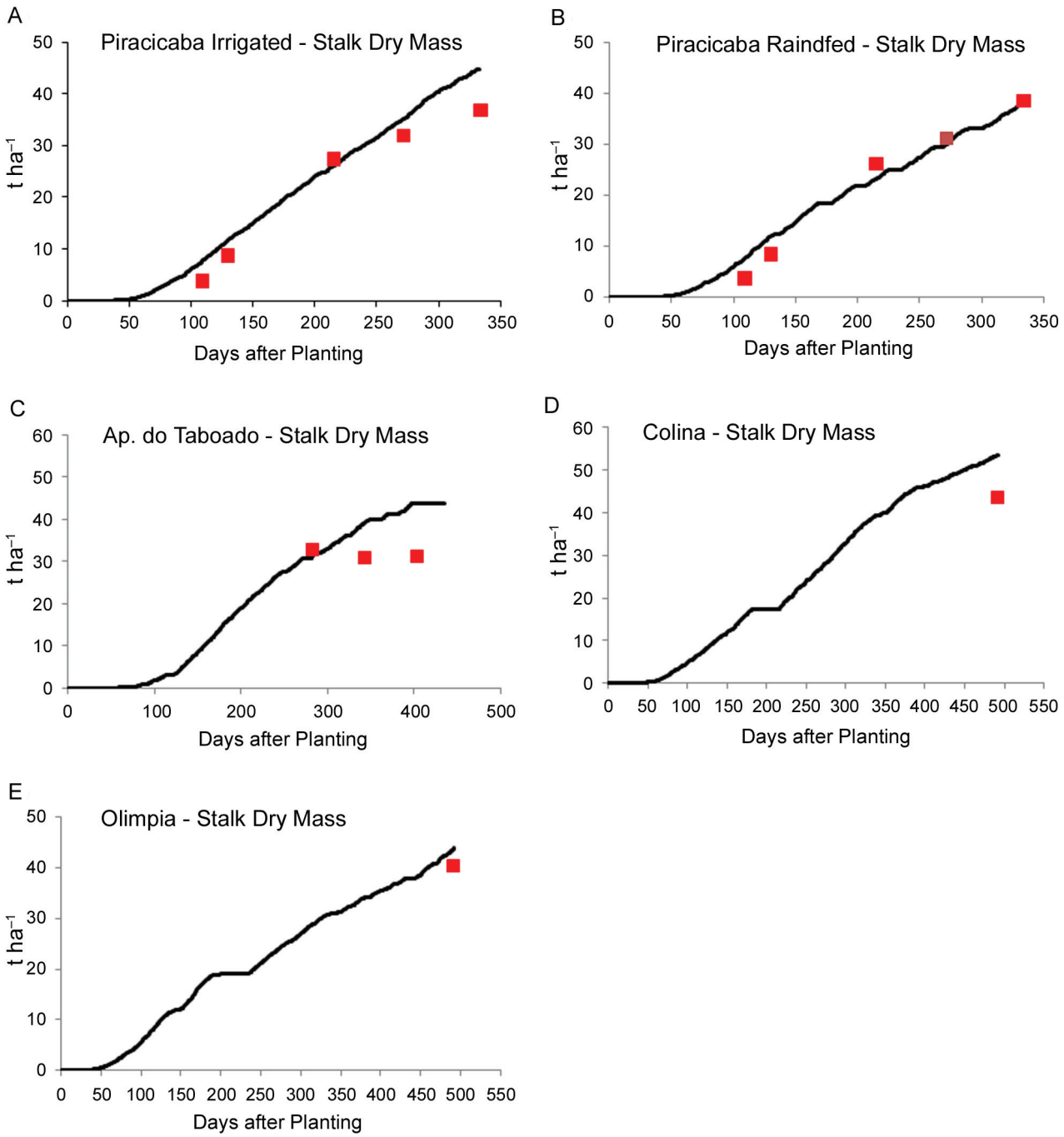


Figure 7 – Time variation of observed and simulated stalk dry mass for five datasets of cultivar SP83-2847, using optimized parameters from Table 2.

In part, the sucrose results might be attributed to its the measurements only being performed during the late season, which reduced the range of variation in the analyzed values (Figure 9b). As modeling efficiency represents how much better the model is compared to the average of observed values, the low efficiency values are primarily due to the time-stable measurements of sucrose content. In general, modeling sucrose accumulation remains a challenge due to the poor understanding of this variable at the whole-plant level (Inman-Bamber et al., 2009). However, the decreased agreement obtained for sucrose (Figure 9b) may be partially due to the characteristics of the measured data rather than to a weakness in the model algorithm.

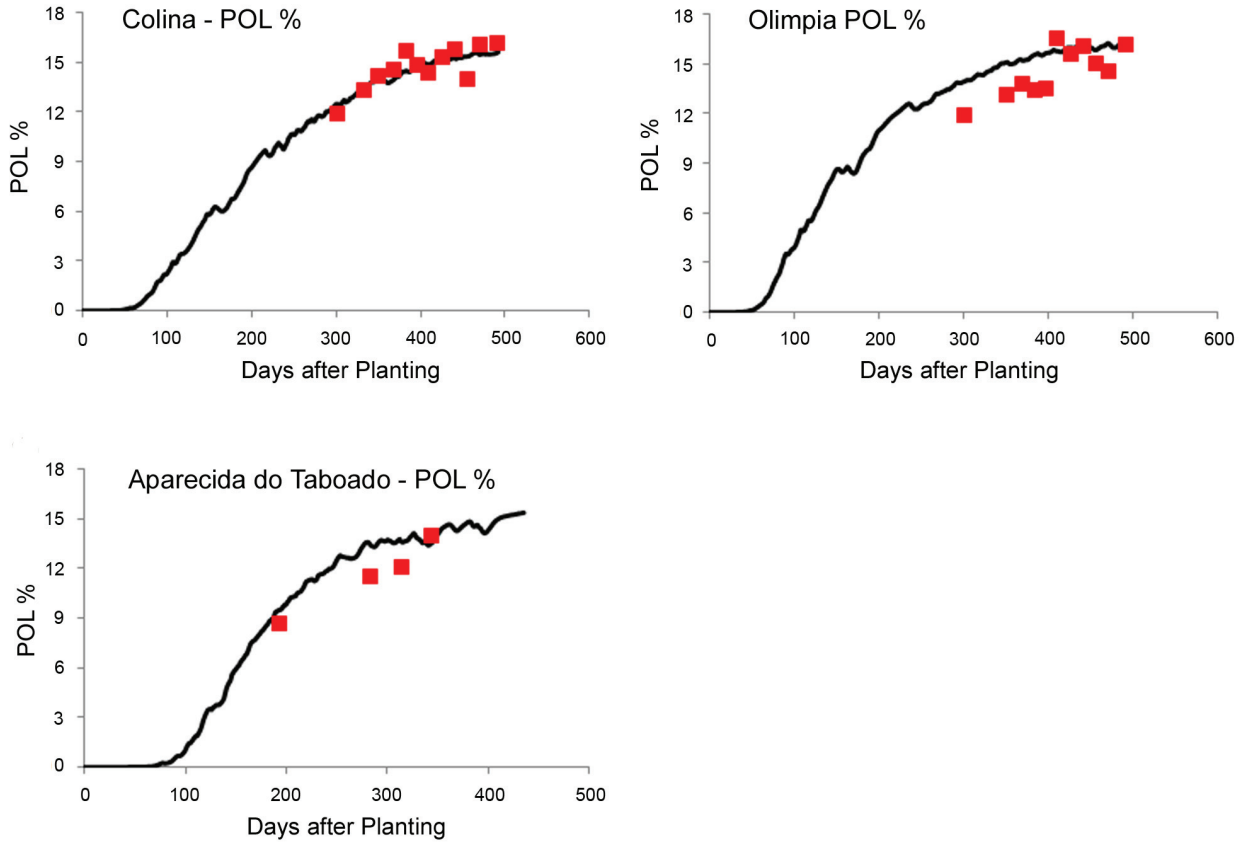


Figure 8 – Time variation of simulated and observed sucrose content for three datasets of cultivar SP83-2847, using optimized parameter from Table 2.

## Conclusions

The model provided a reasonable explanation of the growth of the sugarcane in the analyzed experiments. The calibration using GLUE coupled with the cross-validation technique permits the use of diverse datasets that would be difficult to be used separately because of the heterogeneity of measurements and different measurement strategies. This technique also allowed the richness of this variability to contribute to calibration. The model well simulated sugarcane growth and production under water-limited and irrigated conditions in Southern Brazil. The simulation errors compared well to those of other models reported in the literature for the tested conditions. Fitted leaf development and sucrose accumulation algorithms well represented such processes and agreed with observed data.

## Acknowledgements

To Dr. Frederick Royce and Dr. Cheryl Porter, from the University of Florida, Dr. Abraham Singels, from the South African Sugarcane Research Institute (SASRI), and Dr. Peter Thorburn, from CSIRO Ecosystem Sciences, for the insights and cooperation during the model development. This research was partially supported by Brazilian Council for Scientific and Technological Development (CNPq) through the protocols 302872/2012-4 and 480702/2012-8.

## References

Allen, R.G.; Pereira, L.S.; Raes, D.; Smith, M. 1998. Crop Evapotranspiration: Guidelines for Computing Crop Water Requirements. FAO, Rome, Italy. (Irrigation and Drainage Paper, 56).

Allison, J.C.S.; Pammenter, N.W.; Haslam, R.J. 2007. Why does sugarcane (*Saccharum* sp. hybrid) grow slowly? South African Journal of Botany 73: 546-551.

Ball-Coelho, B.; Sampaio, E.V.S.B.; Thessen, H.; Stewart, J.W.B. 1992. Root dynamics in plant and ratoon crops of sugarcane. Plant Soil 142: 297-305.

Barnes, A.C. 1964. The Sugarcane, Botany, Cultivation, and Utilization: L. Hill, London, UK.

Beven, K.; Binley, A. 1992. The future of distributed models: model calibration and uncertainty prediction. Hydrological Processes 6: 279-298.

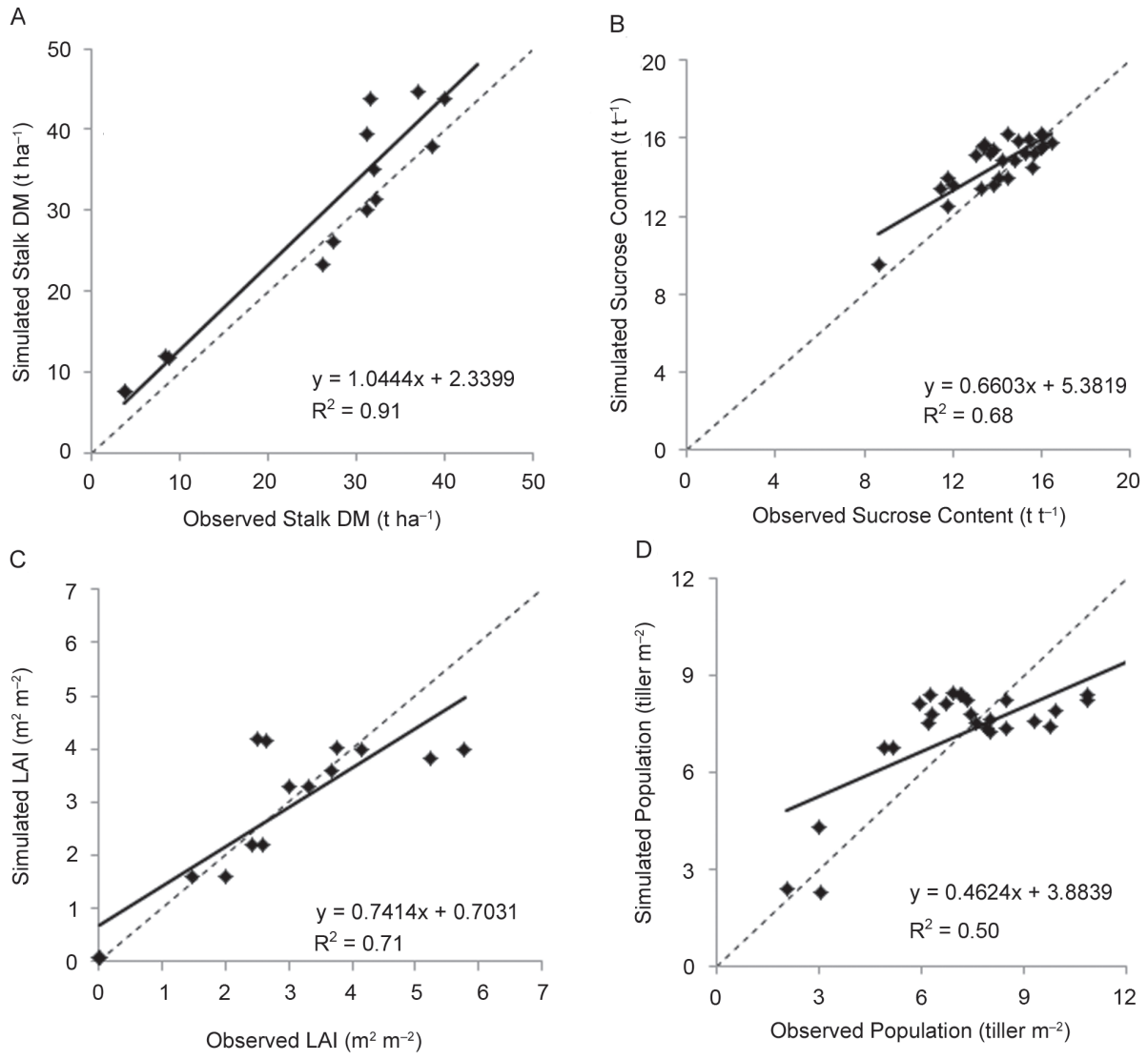


Figure 9 – Simulated values using the optimized parameter set versus observed for (A) stalk dry mass, (B) sucrose content, (C) leaf area index, and (D) tiller population.

Bezuidenhout, C.N.; O'Leary, G.J.; Singels, A.; Bajic, V.B. 2003. A process-based model to simulate changes in tiller density and light interception of sugarcane crops. Agricultural Systems 76: 589-599.

Boote, K.J.; Jones, J.W.; Hoogenboom, G. 1998. Simulation of crop growth: CROPGRO model. p. 651-692. In: Peart, R.M.; Curry, R.B. Agricultural systems modeling and simulation. Marcel Dekker, New York, NY, USA.

Buckingham, E. 1907. Studies on Movement of Soil Moisture. USDA, Washington, DC, USA. (Bulletin, 38).

Campbell, G. 1990. Derivation of an angle density function for canopies with ellipsoidal leaf angle distributions. Agricultural and Forest Meteorology 49: 173-176.

Candela, A.; Noto, L.V.; Aronica, G. 2005. Influence of surface roughness in hydrological response of semiarid catchments. Journal of Hydrology 313: 119-31.

Cheeroo-Nayamuth, F.C.; Robertson, M.J.; Wegener, M.K.; Nayamuth, A.R.H. 2000. Using a simulation model to assess potential and attainable sugarcane yield in Mauritius. Field Crops Research 66: 225-243.

Chopart, J.L.; Rodrigues, S.R.; Azevedo, M.C.B.; Conti, M.C. 2008. Estimating sugarcane root length density through root mapping and orientation modelling. Plant Soil 313: 101-112.

Franks, S.W.; Gineste, P.H.; Beven, K.J.; Merot, P.H. 1998. On constraining the predictions of a distributed model: the incorporation of fuzzy estimates of saturated areas into the calibration process. Water Resources Research 34: 787-797.

He, J.; Dukes, M.D.; Jones, J.W.; Graham, W.D.; Judge, J. 2009. Applying GLUE for estimating CERES-Maize genetic and soil parameters for sweet corn production. Transactions of the ASABE 52: 1907-1921.

He, J.; Jones, J.W.; Graham, W.D.; Dukes, M.D. 2010. Influence of likelihood function choice for estimating crop model parameters using the generalized likelihood uncertainty estimation method. Agricultural Systems 103: 256-264.

He, J.; Dukes, M.D.; Hochmuth, G.J.; Jones, J.W.; Graham, W.D. 2012. Identifying irrigation and nitrogen best management practices for sweet corn production on sandy soils using CERES-Maize model. Agricultural Water Management 109: 61-70.

Inman-Bamber, N.G. 1991. A growth model for sugarcane based on a simple carbon balance and the CERES-Maize water balance. South African Journal of Plant Soil 8: 93-99.

Inman-Bamber, N.G. 1994. Temperature and seasonal effects on canopy development and light interception of sugarcane. Field Crops Research 36: 41-51.

Inman-Bamber, N.G.; Bonnett, G.D.; Spillman, M.F.; Hewitt, M.L.; Jackson, J. 2008. Increasing sucrose accumulation in sugarcane by manipulating leaf extension and photosynthesis with irrigation. Australian Journal of Agricultural Science 59: 13-26.

Inman-Bamber, N.G.; Bonnett, G.D.; Spillman, M.F.; Hewitt, M.L.; Xu, J. 2009. Source–sink differences in genotypes and water regimes influencing sucrose accumulation in sugarcane stalks. Crop and Pasture Science 60: 316-327.

Irvine, J.E. 1975. Relations of photosynthetic rates and leaf and canopy characters to sugarcane yield. Crop Science 15: 671.

Jones, C.A.; Kiniry, J.R. 1986. CERES-Maize: A Simulation Model of Maize Growth and Development. Texas A&M University Press, College Station, TX, USA.

Jones, C.A.; Bland, W.L.; Ritchie, J.T.; Williams, J.R. 1991. Simulation of root growth. p. 91-123. In: Hanks, R.J.; Ritchie, J.T., ed. Modeling plant and soil systems. ASA- CSSA- SSSA, Madison, WI, USA. (Agronomy Monographs, 31).

Jones, C.A.; Wegener, M.K.; Russell, J.S.; McLeod, I.M.; Willians, J.R. 1989. AUSCANE, Simulation of Australian Sugarcane with EPIC. CSIRO, Brisbane, Australia.

Jones, J.W.; Jianqiang, H.; Boote, K.J.; Wilkens, P.; Porter, C.H.; Hu, Z. 2011. Estimating DSSAT cropping system cultivar-specific parameters using bayesian techniques. In: Ahuja, L.; Ma, L., eds. Methods of introducing system models into agricultural research. ASA- CSSA- SSSA, Madison, WI, USA.

Keating, B.A.; Robertson, M.J.; Muchow, R.C.; Huth, N.I. 1999. Modelling sugarcane production systems. I. Description and validation of the sugarcane module. Field Crops Research 61: 253-271.

Kendy, E.; Gerard-Marchant, P.; Walter, M.T.; Zhang, Y.; Liu, C.; Steenhuis, T.S. 2003. A soil-water-balance approach to quantify groundwater recharge from irrigated cropland in the North China Plain. Hydrological Processes 17: 2011-2031.

Laclau, P.; Laclau, J. 2009. Growth of the whole root system for a plant crop of sugarcane under rainfed and irrigated environments in Brazil. Field Crops Research 114: 351-360.

Langellier, P.; Martine, J.F. 2007. Crop modelling assessment of the potential regional irrigated sugarcane production increase. Sugarcane International 25: 8-12.

Liu, D.L.; Bull, T.A. 2001. Simulation of biomass and sugar accumulation in sugarcane using a process-based model. Ecological Modeling 144: 181-211.

Marin, F.R.; Jones, J.W.; Royce, F.; Suguitani, C.; Donzeli, J.L.; Pallone Filho, W.J.; Nassif, D.S.P. 2011. Parameterization and evaluation of predictions of DSSAT/CANEGRO for Brazilian sugarcane. Agronomy Journal 103: 304-315.

McCree, K.J. 1974. Equations for the rate of dark respiration of white clover and grain sorghum, as functions of dry weight, photosynthetic rate, and temperature. Crop Science 14: 509-514.

Nassif, D.S.P.; Marin, F.R.; Pallone Filho, W.J.; Resende, R.S.; Pellegrino, G.Q. 2012. Parameterization and evaluation of the DSSAT/CANEGRO model for Brazilian sugarcane varieties. Pesquisa Agropecuária Brasileira 47: 311-318 (in Portuguese, with abstract in English).

O'Callaghan, J.R.; Hossain, A.H.M.S.; Dahab, M.H.; Wyseure, G.C.L. 1994. SODCOM: a solar driven computational model of crop growth. Computers and Electronics in Agriculture 11: 293-308.

Parton, W.J.; Logan, J.A. 1981. A model for diurnal variation in soil and air temperature. Agricultural Meteorology 23: 205-216.

Pereira, A.R.; Machado, E.C. 1986. A dynamic simulator for sugarcane growth. Bragantia 45: 107-122 (in Portuguese, with abstract in English).

Poulsen, T.G.; Moldrup, P.; Yamaguchi, T.; Schjønning, P.; Hansen, J.A. 1999. Predicting soil-water and soil-air transport properties and their effects on soil-vapor extraction efficiency. Ground Water Monitoring & Remediation 19: 61-70.

Priestley, C.H.B.; Taylor, R.J. 1972. On the assessment of surface heat flux and evaporation using large-scale parameters. Monthly Weather Review 100: 81-92.

Reichardt, K.N.; Nielsen, D.R.; Biggar, J.W. 1971. Scaling of horizontal infiltration into homogeneous soils. Soil Science Society of America Journal 36: 241.

Ritchie, J.T. 1998. Soil water balance and plant water stress. p. 41-53. In: Tsuji, G.Y.; Hoogenboom, G.; Thornton, P.K., eds. Understanding options for agricultural production. Kluwer Academic, Dordrecht, Netherlands.

Robertson, M..J.; Wood, A.W.; Muchow, R.C. 1996. Growth of sugarcane under high input conditions in tropical Australia. I. Radiation use, biomass accumulation and partitioning. Field Crops Research 48: 11-25.

Romanowicz, R.J.; Beven, K.J. 2006. Comments on generalized likelihood uncertainty estimation. Reliability Engineering & System Safety 91: 1315-1321.

Royce, F. 2010. Sugarcane Genotype Coefficients for CASUPRO Model: DSSAT v 4.5. University of Florida, Gainesville, FL, USA.

Sinclair, T.R.; Gilbert, R.A.; Perdomo, R.E.; Shine, J.M.; Powell, G.; Montes, G. 2004. Sugarcane leaf area development under field conditions in Florida, USA. Field Crops Research 88: 171-178.

Silva, D.K.T.; Daros, E.; Zambon, J.L.C.; Weber, H.; Ido, O.T.; Zuffellato-Ribas, K.C.; Koehler, H.S.; Oliveira, R.A. 2005. Growth analysis of ratoon crops of sugarcane cultivars in the northwest of Paraná state in the season 2002/2003. Scientia Agraria 6: 47-53 (in Portuguese, with abstract in English).

Singels, A.; Bezuidenhout, C.N. 2002. A new method of simulating dry matter partitioning in the CANEGRO sugarcane model. Field Crops Research 78: 151-164.

Singels, A.; Jones, M.; van der Berg, M. 2008. DSSAT v4.5-CANEGRO Sugarcane Plant Module: Scientific Documentation. South African Sugarcane Research Institute, Mount Edgecombe, South Africa.

Smith, D.M.; Inman-Bamber, N.G.; Thorburn, P.J. 2005. Growth and function of the sugarcane root system. Field Crops Research 92: 169-183.

Teh, C. 2006. Introduction to Mathematical Modeling of Crop Growth: How the Equations are Derived and Assembled into a Computer Model. BrownWalker Press, Boca Raton, FL, USA.

Thorburn, P.J.; Meier, E.A.; Probert, M.E. 2005. Modelling nitrogen dynamics in sugarcane systems: recent advances and applications. Field Crops Research 92: 337-352.

Tomasella, J.; Hodnett, M.G.; Rossato, L. 2000. Pedotransfer functions for the estimation of soil water retention in Brazilian soils. Soil Science Society of America Journal 64: 327-338.

Uys, L.; Botha, F.C.; Hofmeyr, J.H.S.; Rohwer, J.M. 2007. Kinetic model of sucrose accumulation in maturing sugarcane culm tissue. Phytochemistry 68: 2375-2392.

van Dillewijn, C. 1952. Botany of Sugarcane. Chronica Botanica, Waltham, MA, USA.